ELSEVIER

1 February 1995

Optics Communications 114 (1995) 211–218

OPTICS COMMUNICATIONS

One-dimensional error-diffusion technique adapted for binarization of rotationally symmetric pupil filters

Marek Kowalczyk [1], Manuel Martínez-Corral, Tomasz Cichocki [1], Pedro Andrés

Departamento de Optica, Universidad de Valencia, 46100 Burjassot, Spain

Received 4 August 1994

Abstract

Two novel algorithms for the binarization of continuous rotationally symmetric real and positive pupil filters are presented. Both algorithms are based on the one-dimensional error diffusion concept. In our numerical experiment an original gray-tone apodizer is substituted by a set of transparent and opaque concentric annular zones. Depending on the algorithm the resulting binary mask consists of either equal width or equal area zones. The diffractive behavior of binary filters is evaluated. It is shown that the filter with equal width zones gives Fraunhofer diffraction pattern more similar to that of the original gray-tone apodizer than that with equal area zones, assuming in both cases the same resolution limit of device used to print both filters.

1. Introduction

The amplitude transmittance of pupil filters is usually a continuous rotationally symmetric real function [1]. The fabrication of filters with such a transmittance is still troublesome. It requires sophisticated techniques, like for example photographic registration or vacuum deposition through rotating masks [1,2] or fabrication of a zero-power doublet with one absorbing component [3]. An alternative solution is an approximation of the continuous-tone filter with a binary filter which can be printed, for example, by a digital plotter [4]. The proper choice of binarization algorithm is required to minimize the influence of binarization noise on diffractive behavior of binary filter and in particular on central lobes of its amplitude impulse response (AIR).

Existing digital halftoning algorithms are usually executed on rectangular or hexagonal grid of pixels [5]. Therefore, when we deal with the binarization of a rotationally symmetric filter using such grids, another kind of degradation of its AIR appears, namely, the loss of rotational symmetry. Three binarization methods which preserve the rotational symmetry were proposed by Hegedus [6]. Depending on the method, the pupil area was divided into concentric annular zones of either equal area or equal width or into annular zones with the adapted width. Then, each equal-area zone (EAZ) and equal-width zone (EWZ) was divided into three annular subzones, the inner and the outer opaque, and the middle transparent. The inner and outer radii of transparent annulus were determined by the constraint of transmitting the same energy as the corresponding zone of the continuous-tone pupil filter. In adaptive method binary value of transmittance was changed from 1 to 0 or vice versa as to maintain the integral transmittance of the already binarized part of filter approximately equal to the integral transmittance of the same part of gray-tone filter. Since in each case outer and inner radii of binary zones are strictly determined by the corre-

[1] Permanent address: Institute of Geophysics, Warsaw University, Pasteura 7, 02 093 Warsaw, Poland.

SSDI 0030-4018(94)00607-5

sponding set of equations, these methods required, in principle, arbitrary high resolution of printing device (even for a small number of zones), unless the annuli were plotted on a greatly enlarged scale. The main drawbacks of the latter method are resolution, precision and speed of the plotter, accuracy of the photoreduction steps, and the lengthy fabrication due to multistep process.

In this paper we present two binarization methods which are based on the extensively studied classical version of error diffusion (ED) algorithm [7]. Whereas the generalized ED algorithm is particularly well suited to control the spectral distribution of binarization noise over all the spatial frequency plane, its original version, both one-dimensional (1D) and two-dimensional (2D), has a blue noise characteristic, i.e. the binarization noise contains only high frequency components [8]. Therefore, a strong resemblance between the low frequency spectra of binary filter and its gray-tone counterpart is supposed to be preserved when the classical ED is used as the binarization method. In our modification of the ED algorithm, binary values of transmittance are assigned to concentric annular zones of either equal area or equal width, so that the rotational symmetry of pupil filter and its AIR are preserved. Unlike in the case of Hegedus algorithms, we assign a binary value to the whole EAZ or EWZ because our zones are not subdivided. In this way the width of the zone (in EWZ case) or the width of the finest zone (in EAZ case) can be directly imposed by the resolution limit of printing device – the input parameter of our method. Therefore the binary filters whose transmittance is calculated with the algorithms we present here, can be plotted directly to scale by a high-precision laser writer [9], thus eliminating photoreduction steps.

In our numerical experiment we evaluate the resemblance of the AIRs of EAZ and EWZ binary apodizing filters to the AIR of the corresponding gray-tone filter for different resolution limits of printing device. In the case of the EWZ apodizer we also examine the influence of the direction of execution of ED algorithm (from the pupil center to the edge or vice versa) on its diffractive behavior.

2. One-dimensional error-diffusion algorithm

The ED algorithm was originally introduced by Floyd and Steinberg [7], for the binarization of pictures. The general description of this algorithm can be found elsewhere (see for example Ref. [5]). In our work we are interested in its 1D version with only one weight, which can be described in the following way. From a given normalized continuous function $f(x)$ the normalized sampled distribution $f(i)$, $i=0, \ldots, N-1$, is obtained, which we will refer to as normalized input function. The first input value $f(0)$ is compared with a threshold t_0 and the binary output is set to 1 or 0, depending on whether $f(0)$ is larger or smaller than t_0. In general t_0 can be a function of i [10]. In our formulation we put $t_0=0.5$. The hard-clip operation results in an error term $e(0)=b(0)-f(0)$, being $b(0)$ the first binary assignment. This error term is then multiplied by a weighting factor $w(1)$ and subtracted from the next input value $f(1)$. The modified input value $f(1)-w(1)e(0)$ is then compared with the threshold to give the next output value $b(1)$. The coefficient $w(1)$ indicates the fraction of the error $e(0)$ transferred to $f(1)$. Binary value assigned to ith sample can be written as

$$b(i)=\text{step}[f(i)-w(i)e(i-1)-0.5]\,, \qquad (1)$$

where step [ ] function is defined as zero when its argument is negative and 1 if otherwise. The algorithm binarizes and corrects sequentially all the samples of the input function. However, the error obtained in the last sample, $e(N-1)$, remains not corrected.

In the original 1D ED method it is usual to put $w(i)=1$. We will show here that this may lead to improper results if 1D ED is applied to binarization of 2D pupil functions with rotational symmetry.

3. Binarization of two-dimensional functions

The 1D ED algorithm can be applied to binarize 2D functions when used with respect to rotationally symmetric functions, i.e. functions whose value depends only on the radial coordinate. In such a case the resulting binary output consists of a set of concentric transparent and opaque annular zones. However some modifications of the ED algorithm are

necessary for obtaining an optimal binarization, that is for obtaining a high degree of similarity between the spectra of continuous function and its binary version. Let us show it in the following reasoning in which we compare the diffractive behavior of a 2D binary filter obtained with either 2D ED or 1D ED algorithm, assuming in both cases rotational symmetry of continuous-tone pupil filter.

When a 2D continuous function is binarized by the 2D ED algorithm, a matrix of transparent and opaque rectangular cells is obtained. The contribution, E_{ij}, of an arbitrary rectangular cell, Σ_{ij}, of the binary filter to the field amplitude at the axial point of its Fraunhofer diffraction pattern is, apart from a constant factor,

$$E_{ij}=b(i,j)\int\limits_{\Sigma_{ij}}\int \mathrm{d}x\,\mathrm{d}y=b(i,j)\,S(i,j)\,, \tag{2}$$

where $b(i,j)$ is the binary transmittance assigned to the corresponding reactangular cell, whereas $S(i,j)$ represents the area of the cell.

On the other hand, if the 2D rotationally symmetric filter is binarized by the 1D ED algorithm, the contribution, E_i, of the ith annular binary zone to the central point of the Fraunhofer pattern is

$$E_i=2\pi b(i)\int\limits_{r_i}^{r_{i+1}} r\,\mathrm{d}r=b(i)\pi(r_{i+1}^2-r_i^2)=b(i)S(i)\,,$$

$$i=0,1,2,\ldots,N-1\,, \tag{3}$$

where r_i is the inner radius of ith annular zone ($r_0\equiv 0$), $b(i)$ is the binary value of amplitude transmittance assigned to the annular zone, and $S(i)$ represents the area of the zone. Thus, the value of E_i is proportional to the volume under the binary function within the ith annular zone.

Note that in Cartesian coordinates all the binary cells are rectangular and usually they have the same area. Then, their relative contribution to the integral transmittance depends only on the assigned binary value, $b(i,j)$. However, in polar coordinates the contribution of an annular zone depends not only on the assigned binary value, $b(i)$, but also on the difference $(\pi r_{i+1}^2-\pi r_i^2)$, i.e. on the area of the zone which varies proportionally to $(r_{i+1}+r_i)$ when $(r_{i+1}-r_i)=$ const (EWZ). Thus, when the 1D ED algorithm with $w(i)\equiv 1$ is applied directly to binarization of rotationally symmetric filters it can lead to improper results, because the error obtained in one zone is then spread over a zone whose area may be different from one it originated. To overcome this problem we propose either to divide the pupil into annular zones of equal area, or to weight the error, $e(i-1)$, to be diffused to the ith zone by the coefficient

$$w(i)=\frac{S(i-1)}{S(i)}=\frac{r_i^2-r_{i-1}^2}{r_{i+1}^2-r_i^2}\,, \tag{4}$$

which is equal to the ratio of the area of already binarized zone and that under binarization.

3.1. Annuli of equal width

In order to binarize the amplitude transmittance, $T(r)$, of a rotationally symmetric pupil filter by means of 1D ED algorithm, the natural way of division of the area of the pupil into binary cells is by dividing it into a set of concentric EWZs. Let us assume that our plotter is able to draw N EWZs within the unit-radius pupil. Thus, the inner radius of the ith annular zone is

$$r_i=i/N\,. \tag{5}$$

The width of the each zone, Δ_w, is equal to $1/N$ whereas the area of the ith zone is

$$S(i)=\pi(r_{i+1}^2-r_i^2)=\pi\frac{2i+1}{N^2}\,. \tag{6}$$

As is stated above, the influence of an arbitrary ith zone on the integral transmittance depends on the volume of the zone. Then, the sampling must be performed at the circle

$$\tilde{r}_i=\frac{1}{N}\sqrt{\frac{i^2+(i+1)^2}{2}}\,, \tag{7}$$

that divides the zone into two parts of equal area.

In this sampling it is tacitly assumed that with change of variables $\zeta=\pi r^2$, the amplitude transmittance $T(r)$ is approximately linear as a function of ζ within the interval $[\zeta_i,\zeta_{i+1}]$, where $\zeta_i=\zeta(r_i)$. If this assumption is not a good approximation, the sampling should be done at $\tilde{r}_i$ such that

$$T(\tilde{r}_i)=\frac{2\pi}{S(i)}\int\limits_{r_i}^{r_{i+1}} T(r)\,r\,\mathrm{d}r\,. \tag{8}$$

Along the circle of the radius $\tilde{r}_i$ the function $T(r)$ takes on its mean value over the ith annular zone $[r_i, r_{i+1}]$. In practice we do not look for $\tilde{r}_i$ defined by Eq. (8), although it exists according to the first low of the mean for integrals. We simply assign $T(\tilde{r}_i)$ given by Eq. (8) to the ith annular zone.

Taking into account Eqs. (4) and (6), the diffusion weight can be rewritten as

$$w(i)=\frac{2i-1}{2i+1}. \tag{9}$$

3.1.1. Direction of the binarization process

When the binarization with EWZs is dealt with, the direction of the binarization process is supposed to affect the result. If the procedure starts from $i=0$, i.e. from the center of the filter, the error obtained at the last sample, $i=N-1$, remains uncorrected. Note that the outermost annulus has the biggest area, hence the influence of its noncorrected error on the integral transmittance can be significant. In order to minimize the noncorrected error, we propose to process the algorithm in the opposite direction, that is starting from $i=N-1$. In such a case the diffusion weight, $w'(i)$, is defined as

$$w'(i)=\frac{S(i+1)}{S(i)}=\frac{1}{w(i+1)}. \tag{10}$$

As we will verify in a numerical experiment, the diffractive behavior of binary filters obtained in this way is better than that of filters obtained by the ordinary direction of binarization.

3.2. Annuli of equal area

Another approach to binarization of rotationally symmetric pupil filters is that in which diffusion weights given by Eq. (4) are identically equal to unity. We can meet this condition if we divide the pupil area into M annular EAZs. The inner radius of ith annulus is equal to

$$r_i=\sqrt{i/M}, \tag{11}$$

where again the unit radius of the pupil is assumed. The area of each annulus is constant and equal to

$$S(i)=\pi(r_{i+1}^2-r_i^2)=\pi/M. \tag{12}$$

Hence, $w(i)\equiv 1$ during the whole binarization process. The sampling of $T(r)$ must be done at

$$\tilde{r}_i=\sqrt{\frac{2i+1}{2M}}. \tag{13}$$

The comment that we made after Eq. (8) is valid also in this case. The width Δ_A of the finest, i.e. the outermost zone is

$$\Delta_A=1-r_{M-1}=1-\sqrt{1-1/M}. \tag{14}$$

From the condition $\Delta_A=\Delta_W$ it results that

$$M=\frac{N^2}{2N-1}\cong\frac{N}{2}. \tag{15}$$

Thus, with the printing device which is able to print N EWZs we can print at most $N^2/(2N-1)$ EAZs. If we realize that for $M=50$ the zone number $M-2$ (the zone next to the finest one) is wider than Δ_A by only one percent, it will be clear that in order to draw such an EAZ mask we must use a digital plotter characterized by a high relation of the smallest marking size to the accuracy with which it can position the output.

There is a close correspondence between 1D ED with EAZs and the classical version of 1D ED algorithm. These algorithms became formally identical if the pupil function is represented as a function of ζ instead of r. In fact, it results from Eqs. (11) and (13) that with this mapping the graph of the pupil function consists of equal-width segments and sampling values used in ED algorithm are taken in the central point of each segment.

4. Numerical experiment

To study the performance of proposed algorithms we carried out a computer experiment in which an apodizing pupil was binarized. As a pupil function we chose a truncated Bessel function of the first kind, zero order [1]

$$\begin{aligned} T(r)&=J_0(\chi_1 r), \quad r\leqslant 1,\\ &=0, \qquad\qquad r>1, \end{aligned} \tag{16}$$

where $\chi_1=2.405$ is the first positive root of the equation $J_0(\chi)=0$. Among all the apodizing pupil functions which provide the same energy flux through the pupil, that of Eq. (16) minimizes the second mo-

ment of the intensity distribution in the Fraunhofer diffraction pattern [11].

The AIRs of calculated binary filters were computed and compared with those of continuous-tone apodizer in terms of signal to noise ratio (SNR):

$$\mathrm{SNR}(K) = \int_A [F(u,v)]^2 \,\mathrm{d}u\,\mathrm{d}v \times \left(\int_A [F(u,v) - G(u,v;K)]^2 \,\mathrm{d}u\,\mathrm{d}v \right)^{-1}, \qquad (17)$$

where $F(u, v)$ represents the intensity distribution in the Fraunhofer diffraction pattern of the continuous-tone function, $G(u, v; K)$ the intensity distribution in the Fraunhofer diffraction pattern of the binary function whose domain consists of K annular cells, and A an area in the Fourier domain. In our experiment A was a circle centered on the optical axis and extended up to the second minimum of continuous-tone filter Fraunhofer diffraction pattern.

The results of numerical experiments are shown in Figs. 1 and 2. Fig. 1 presents SNR versus number of annuli constituting an EWZ filter for the two directions of binarization process. The figure shows that binary filters generated with the EWZ algorithm processed from the edge to the center of the pupil (square symbols) provide, in general, higher values of SNR. Fig. 2 illustrates the SNR(M) dependence in the EAZ case. In both cases the SNR is high even for binary filters consisting of a few annuli.

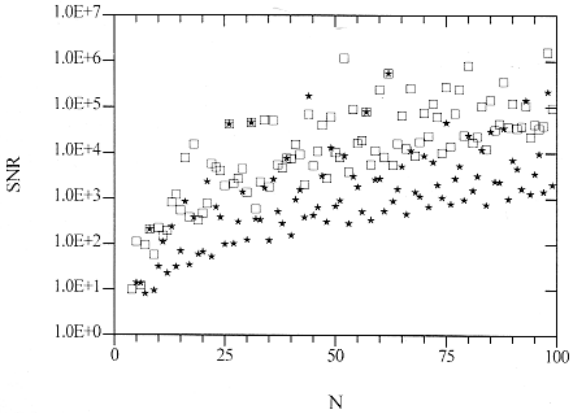

Fig. 1. SNR versus number of annuli for binary filters obtained with EWZ algorithm processed from the edge to the center of the pupil (square symbols), and in the opposite direction (star symbols).

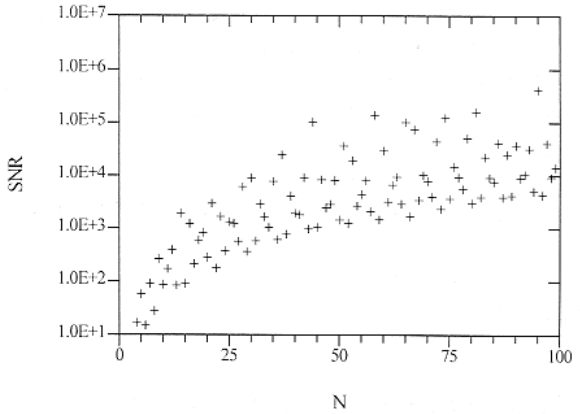

Fig. 2. SNR versus number of annuli for binary filters obtained with EAZ algorithm.

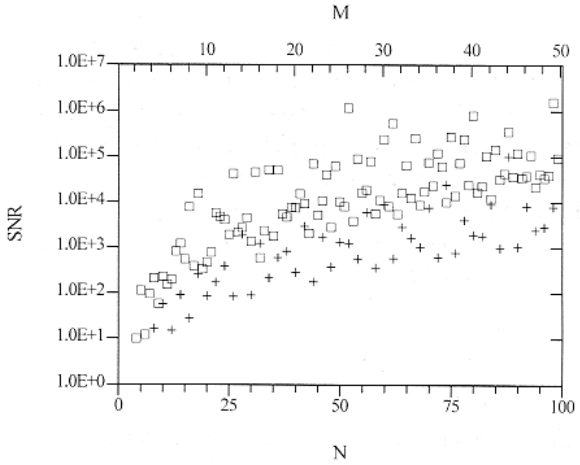

Fig. 3. Comparison of the SNRs obtained with EWZ algorithm (square symbols), and with EAZ algorithm (plus symbols), assuming in both cases the same resolution of printing device. Upper scale corresponds to EAZ filters.

To compare the performance of both proposed algorithms we combine Fig. 1 (square symbols only) and Fig. 2 with changed horizontal scale. It results from Eq. (15) that direct comparison is inadequate when the resolution of the printing device is taken into account. The SNR obtained with a filter of N EWZs should be compared with the SNR of a filter consisting of $M = N^2/(2N-1)$ EAZs. According to this criterion Fig. 3 was prepared, in which EWZ filters show, in general, better diffraction behavior than EAZ ones.

It is seen in Figs. 1 and 2 that in general the SNR increases as the number of zones increases. However,

neither the SNR(N) dependence for EWZ subdivision nor the SNR(M) dependence for EAZ subdivision are monotonic. Some "privileged" numbers of zones appear for which SNR is considerably higher than for slightly smaller or larger N or M. A simple explanation of this phenomenon can be given in the ζ space for the EAZ case as follows. One of the aims of ED procedure when applied to binarization of pupil filters is to maintain unchanged the integral transmittance of the original gray-tone filter. The integral transmittance is equal to the value which the Fourier transform of the pupil function takes on at the origin of the Fourier plane. In this way the central part of the spectrum of binary elements remains unaffected by the binarization process [8]. The integral transmittance of the pupil used in our experiment is equal to $2\chi_1^{-1}J_1(\chi_1)=0.4243\pi\approx 4/3$, where J_1 is a Bessel function of the first kind, first order [1]. This integral transmittance is equal to the area under the continuous curve $J_0(\chi_1\sqrt{\zeta/\pi})$ (and also to the volume under the central lobe of $J_0(\chi_1 r)$), whose binary version is supposed to be built up with M equal boxes of the area π/M each (see Fig.5c). The numbers M which meet best the following equation

$$\frac{4}{3}=\frac{\pi}{M}n, \quad 1\leqslant n\leqslant M \tag{18}$$

or, equivalently,

$$n/M=0.4243\,, \tag{19}$$

where n is the number of clear zones, are particularly well suited for this task. In fact $n/M=3/7=6/14=\ldots=0.4286$ are the best approximate solutions of Eq. (18). It is seen in Fig. 2 that for $M=7, 14, 21, \ldots$ the SNR reaches its local maxima. The absolute maximum does not belong to this series because we calculate the SNR in the area A which covers more than the central part of the main lobe, for which the above reasoning is strictly valid.

In Fig. 4 we present a selected EWZ filter, obtained with relatively low resolution (52 zones), which has a high SNR. Note that the presence of an opaque zone close to the pupil center, where original continuous-tone filter has transmittance close to 1, is related to the direction of the binarization process: it compensates the error made in the outer part of the filter.

In Fig. 5 a selected EAZ filter, obtained with only 44 zones, is shown. Also this filter has a high SNR value.

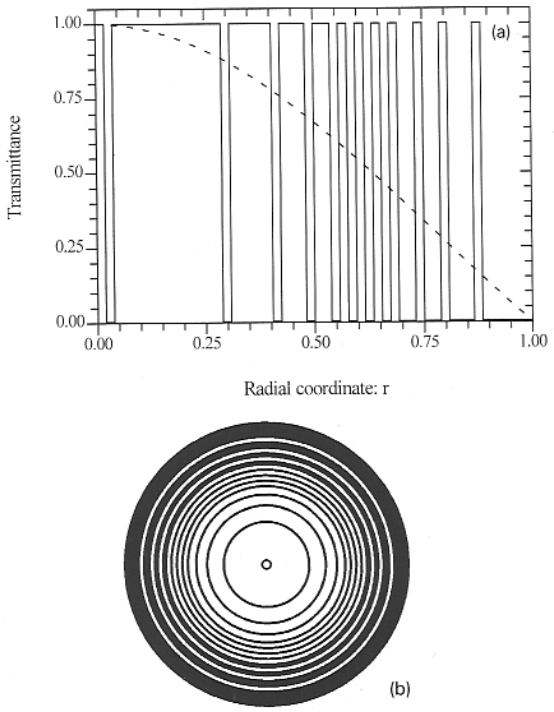

Fig. 4. EWZ binary version of zero-order Bessel filter. ED algorithm executed over 52 annular cells: (a) one-dimensional representation (dashed-line curve represents the amplitude transmittance of continuous-tone filter); (b) actual two-dimensional representation.

The intensity profiles obtained in the Fraunhofer diffraction region of corresponding filters are shown in Fig. 6. The logarithmic scale is used to show the differences between diffraction patterns of the binary and gray-tone filters which appear, first of all, in the side-lobe region. The differences in A region are negligible, which explains the high SNR obtained for these filters.

5. Conclusions

Two new algorithms for binarization of rotationally symmetric apodizers based on one-dimensional (1D) error diffusion (ED) algorithm have been presented. The binary filters obtained with these algorithms consist of concentric transparent and opaque annuli of either equal width or equal area. Owing to

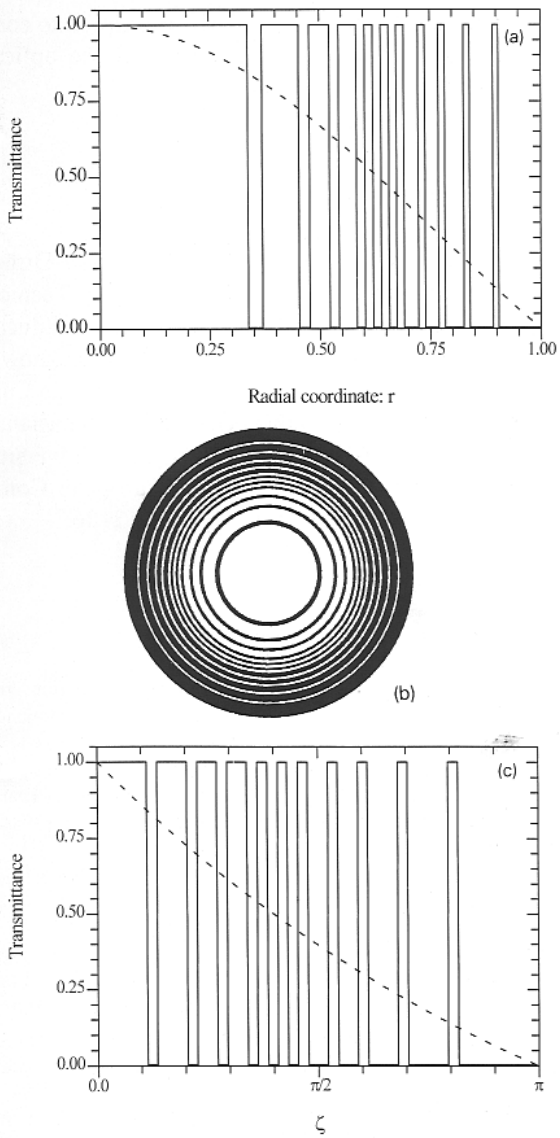

Fig. 5. EAZ binary version of zero-order Bessel filter consisting of 44 annuli: (a) one-dimensional representation; (b) actual two-dimensional representation; (c) ζ-space representation (dashed-line curves represent the amplitude transmittance of continuous-tone filter).

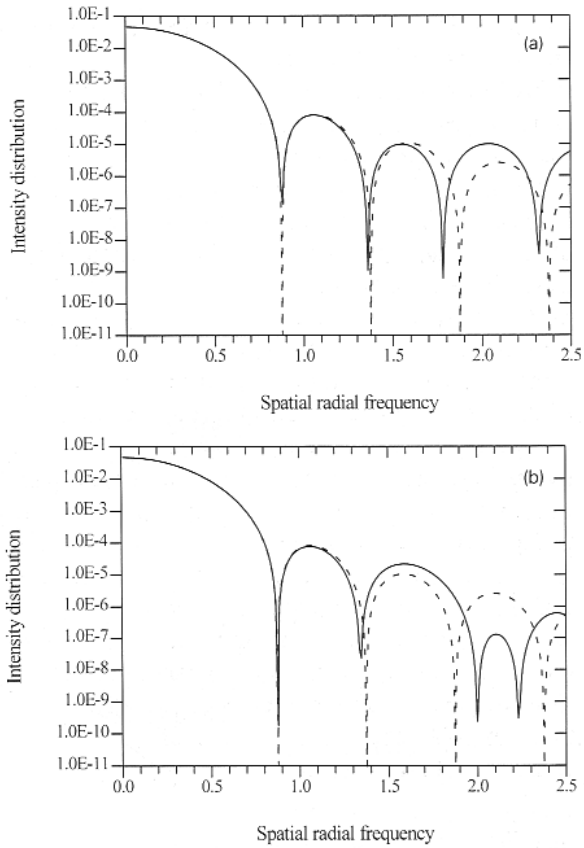

Fig. 6. Cross section of the intensity distribution in the Fraunhofer diffraction pattern of: (a) EWZ binary filter consisting of 52 annuli; (b) EAZ binary filter consisting of 44 annuli. Dashed-line curve represents the diffraction pattern of continuous-tone filter.

the nature of the proposed algorithms, the binary filters present the following features.

(i) The rotational symmetry of the pupil filter and its amplitude impulse response (AIR) are preserved.

(ii) The low frequency spectrum of binary filters remains nearly unaffected by binarization noise. This was proved in terms of signal to noise ratio (SNR) being the quantitative measure of the resemblance between their AIRs and the AIR of the original gray-tone filter.

(iii) The equal-width zone (EWZ) filters are, in general, characterized by higher values of SNR than those obtained with the other method tested in this work. The advantage of these filters is even more evident if the algorithm is processed starting from the sample closest to the edge of the pupil.

(iv) In order to fabricate the resulting binary mask with a printing device, the required resolution is much lower than that required by other binarization methods which divide the pupil into similar number of either equal width or equal area annular zones. The printing devices whose positional accuracy is much higher than the smallest spot size, as for example most

digital plotters, are better suited for this task than laser printers or liquid-crystal devices.

We have also found that the SNR does not increase monotonically as the number of zones of binary filter increases. As a consequence of that, we can state that on designing of binary rotationally symmetric pupil filters, the requirement of spatial resolution as high as possible sometimes should be slightly relaxed in order to provide a good match between the integral transmittance of the filter and the number of its binary zones.

We would like to outline some differences between the binary masks obtained by using the amplitude transmittance of a Fresnel zone plate as a binary carrier of pupil function [12], and those obtained by means of equal-area zone (EAZ) version of 1D ED algorithm presented in this work. The mask which belongs to the former class can be considered a binary Gabor hologram of a two-dimensional (2D) object whose amplitude transmittance is proportional to the AIR in question. Such a hologram is coded by a phase-detour method and is referred to as modulated Fresnel zone plate. When illuminated with a point source it reproduces at each focal plane of the zone plate (except for that of zero order) the amplitude distribution of the recorded object plus bias formed by spherical waves converging towards or diverging from other foci. On the contrary, our EAZ binary filter reproduces in the central part of the focal plane of the illuminating converging spherical wave the Fourier transform of its gray-tone counterpart without bias. The main advantage offered by modulated zone plates is the possibility to code both real and complex pupil functions.

Finally we would like to remark that with the change of variables $\zeta = \pi r^2$ the amplitude distribution along the optical axis is proportional to the 1D Fourier transform of the amplitude transmittance of the filter [13,14]. The above and the well established theory of spectral properties of binary patterns obtained with unit-weight 1D ED algorithm [8,15], make our EAZ filters particularly well suited to control the axial diffractional behavior of the optical system.

Acknowledgements

This work was partially supported by the Dirección General de Investigación Científica y Técnica (grant PB93-0354-CO2-01), Ministerio de Educación y Ciencia, Spain. Marek Kowalczyk acknowledges gratefully a grant from the Consellería de Cultura, Educació i Ciència de la Generalitat Valenciana, Spain. The stay of Tomasz Cichocki at the University of Valencia was sponsored by the European Community grant TEMPUS # IMG-92-PL-2186.

References

[1] P. Jacquinot and B. Roizen-Dossier, Apodisation, in: Progress in Optics, Vol. III, ed. E. Wolf (North-Holland, Amsterdam, 1964).
[2] E.W.S. Hee, Optics and Laser Technology (April 1975) 75.
[3] M. Mino and Y. Okano, Appl. Optics 10 (1971) 2219.
[4] H.S. Watkins and J.S. Moore, IEEE Spectrum 21 (1984) 26.
[5] R. Ulichney, Digital Halftoning (MIT Press, Cambridge, 1987).
[6] Z.S. Hegedus, Optica Acta 32 (1985) 815.
[7] R.W. Floyd and L. Steinberg, Proc. Soc. Inf. Disp. 17 (1976) 75.
[8] S. Weissbach and F. Wyrowski, Appl. Optics 31 (1992) 2518.
[9] S.C. Baber, in: Proc. SPIE, Holographic Optics: Optically and Computer Generated 1052 (1989) 66.
[10] G.S. Fawcett and G.F. Schrack, Proc. Soc. Inf. Disp. 27 (1986) 305.
[11] T. Asakura and T. Ueno, Nouv. Rev. Optique 7 (1976) 199.
[12] A. Engel and G. Herziger, Appl. Optics 12 (1973) 471.
[13] C.J.R. Sheppard and Z.S. Hegedus, J. Opt. Soc. Am. A 5 (1988) 643.
[14] M. Martínez-Corral, P. Andrés and J. Ojeda-Castañeda, Appl. Optics 33 (1994) 2223; and references therein.
[15] R. Eschbach and R. Hauck, Optics Comm. 52 (1984) 165.